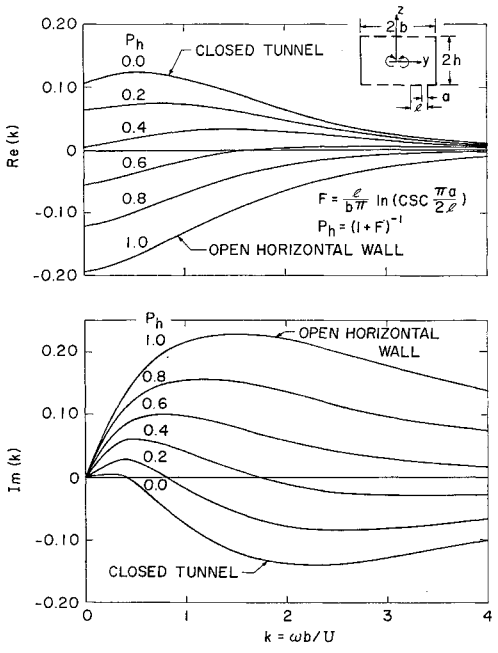

Fig. 2 Upwash interference at the plane of wing in rectangular tunnels with solid side walls of eight-to-width ratio 0.667.

and (3). At the plane of the wing, $x = y = z = 0$, the expression may be simplified to

$$W_{ki}|_0 = (1/b)\partial\phi_{ki}/\partial z|_0 = (s\Gamma_k/2bh)\{Re(k) + iIm(k)\} \quad (15)$$

where

$$Re(k) = \frac{1}{2\pi}\lambda\left\{\sum_{n=1}^{\infty}\frac{k}{n}K_1(2nk) + \frac{\pi}{2}\sum_{m=0}^{\infty} j \times (k^2 + m^2\pi^2)^{1/2} A[(k^2 + m^2\pi^2)^{1/2}]\right\}$$

$$Im(k) = \frac{k}{4}\lambda\left[\sum_{n=1}^{\infty}\frac{I_1(2nk) - L_{-1}(2nk)}{n} + \frac{4}{\pi}\sum_{m=0}^{\infty} j\int_0^{\infty} A(p_m)\frac{p_m}{q^2 - k^2}\,dq\right]$$

$L_{-1}(2nk)$ = Modified Struve function

The real and imaginary parts of the upwash interference relationship, Eq. (15), are plotted against reduced frequency for tunnels of height-to-width ratio $\lambda = 0.667$ in Fig. 2. The results of the static case derived in Ref. 1 may be obtained by taking the limit $k \to 0$ in Eq. (15).

Concluding Remarks

Results are given here for incompressible flow and all frequencies; however, they may be used for low frequencies in subsonic compressible flow with a minor modification, as in Eq. (5). All results are obtained for a small-wing model on the centerline of the tunnel. The expression for a model with an off-centerline position may be derived in a similar manner. Within the assumptions of linearized theory, solutions of any wing configuration may be obtained by superposition since it may be regarded as made up of "small wings," that is, lifting elements of area. The over-all corrections to forces and moments in wind tunnels as for general wings may be calculated[7] by the utilization of the upwash interference.

By examining the curves of the exact solutions given here, the validity of the approximation solution[2] in a power series of frequency up to the first order is within a rather narrow range of small values frequency, if the solution is extended to a slotted-wall tunnel.

The present results for slotted-wall tunnels provide information that will assist in choosing a tunnel wall configuration. For example, the optimum slot parameter of a circular cross section is about $P = 0.6$ from Fig. 1. For rectangular tunnel of height-to-width ratio of 0.667 (Fig. 2), the optimum slot parameter is in the range of $0.4 < P_h < 0.6$.

References

[1] Pindzola, M. and Lo, C. F., "Boundary Interference at Subsonic Speeds in Wind Tunnels with Ventilated Walls," AEDC-TR-69-47, May 1969, Arnold Engineering Development Center, Arnold Air Force Station, Tenn.

[2] Garner, H. C., Moore, A. W., and Wight, K. C., "The Theory of Interference Effects on Dynamic Measurements in Slotted-Wall Tunnels at Subsonic Speeds and Comparisons with Experiment," ARC 28 339, Sept. 1966, National Physical Lab., British.

[3] Watkins, C. E., Runyan, H. L., and Woolston, D. C., "On the Kernel Function of the Integral Equation Relating the Lift and Downwash Distributions of Oscillating Finite Wings in Subsonic Flow," Rept. 1234, 1955, NACA.

[4] Goodman, T. R., "The Upwash Correction for an Oscillating Wing in a Wind Tunnel," *Journal of the Aeronautical Sciences*, Vol. 20, No. 6, June 1953, pp. 383–386 and 406.

[5] Miles, J. W., "On the Compressibility Correction for Subsonic Unsteady Flow," *Journal of the Aeronautical Sciences*, Vol. 17, No. 3, March 1950, p. 181.

[6] Davis, D. D. and Moore, D., "Analytical Study of Blockage and Lift-Interference Corrections for Slotted Tunnels Obtained by the Substitution of an Equivalent Homogeneous Boundary for the Discrete Slots," RM L53E07b, 1953, NACA.

[7] Garner, H. C. et al., "Subsonic Wind Tunnel Wall Corrections," Chap. IV, AGARDograph 109, Oct. 1966.

A Further Note on Shock-Tube Measurements of End-Wall Radiative Heat Transfer in Air

PAUL R. KNOTT,* LELAND A. CARLSON,† AND ROBERT M. NEREM‡
The Ohio State University, Columbus, Ohio

SHOCK-tube measurements of the end-wall radiative heat transfer behind reflected shock waves in air have been previously reported in Ref. 1. These measurements were carried out at an initial shock-tube driven pressure of 1 mm Hg and at shock velocities ranging from 6.5 to 9.5 km/sec. A thin-film heat-transfer gage mounted behind a sapphire window located in the end wall of an arc-driven shock tube was used to measure the radiation in the wavelength region 0.17–6 μ.

In Ref. 1, comparisons were made between the experimental data and end-wall heat-transfer predictions based upon numerical solutions for the flowfield behind reflected shock waves in air. These equilibrium air solutions used several different models to account for radiative emission and absorption. Included were models for a gray gas as well as for a nongray gas. In the latter case, a two-step absorption co-

Received July 14, 1969. The research was supported by the Aerospace Research Laboratories, Office of Aerospace Research, U.S. Air Force, Wright-Patterson Air Force Base, Ohio under Contract No. F33615-68-C-1249.

* Research Assistant, Aeronautical and Astronautical Laboratory.

† Research Assistant, Aeronautical and Astronautical Laboratory. Member AIAA.

‡ Associate Professor, Department of Aeronautical and Astronautical Engineering. Associate Fellow AIAA.

Table 1 Calculated spectral absorption cross sections for five-step model based on nitrogen atom line and continuum radiation

Temperature, °K	Effective radiative cross section for nitrogen atoms, cm²				
	Region 1	Region 2[a]	Region 3	Region 4[a]	Region 5[a]
8,000	5.4237×10^{-22}	2.26×10^{-24}	7.4912×10^{-23}	2.470×10^{-20}	8.17×10^{-16}
10,000	1.104×10^{-20}	6.450×10^{-23}	1.3423×10^{-18}	6.260×10^{-20}	2.46×10^{-16}
12,000	7.656×10^{-20}	6.130×10^{-22}	1.9140×10^{-18}	1.130×10^{-19}	1.18×10^{-16}
14,000	2.9408×10^{-19}	3.23×10^{-21}	2.4063×10^{-18}	1.660×10^{-19}	7.3418×10^{-17}
16,000	7.9117×10^{-19}	1.29×10^{-20}	2.8075×10^{-18}	2.222×10^{-19}	5.3232×10^{-17}
18,000	1.6279×10^{-18}	3.5483×10^{-20}	3.1254×10^{-18}	2.78×10^{-19}	4.2348×10^{-17}
20,000	2.85×10^{-18}	9.677×10^{-20}	3.25×10^{-18}	3.33×10^{-19}	3.545×10^{-17}

[a] These values should be corrected for the photo-ionization edge shift using the results of Armstrong in Ref. 4.

efficient was used in which, for the conditions of the experiment, the vacuum ultra-violet was highly self-absorbed and the visible and infrared relatively transparent. Although general agreement existed, end-wall radiative heat-transfer rates predicted by the two-step absorption coefficient calculations still exceeded the experimental data by as much as 50%.

In order to improve upon the accuracy of such radiative transfer calculations, a five-step absorption coefficient model that is applicable to a temperature range of approximately 8000–20,000°K was recently developed for nitrogen. This corresponds to the range of interest not only in the present reflected shock-wave problem but also in entry radiation calculations. In this new absorption coefficient model, the spectrum was divided into the five following regions: 1) $1.298 \leq h\nu \leq 1.573$ ev; 2) $1.573 < h\nu \leq 7.880$ ev; 3) $7.880 < h\nu \leq 9.550$ ev; 4) $9.550 < h\nu \leq 11.27$ ev; 5) $11.27 < h\nu \leq 20.00$ ev. For regions 1 and 3, the mean absorption coefficient was based solely on the major bound-bound atomic line transitions. Six nitrogen lines were included in region one, while for region 3, five atomic lines were used. In these regions, the mean absorption coefficient was evaluated as

$$k_i = \sum_j B_{\nu j} \int_0^\infty k_\nu d\nu \Big/ \int_i B_\nu d_\nu \qquad (1)$$

where the summation was over all lines included. The integral in the numerator is directly related to the f-number of the line and the nitrogen number density, $B_{\nu j}$ is the black-body intensity at the center of the jth line, and the denominator is the integral of the black-body function over the spectral region in question. In general, NBS[2] f-numbers were used; however, when a value for a particular transition was not available from that source, the f-number value of Wilson and Nicolet[3] was used. It should be noted that although only eleven lines were included in regions 1 and 3, other lines were considered (see Wiese et al.[2] for a tabulation of nitrogen atomic line transitions) and were found to make relatively unimportant contributions within the framework of this model.

The mean absorption coefficient for regions 2, 4, and 5, on the other hand, was based solely on continuum transitions and included only the bound-free and free-free absorption processes involving nitrogen atoms. The associated radiative cross sections were evaluated following the procedure of Wilson and Nicolet[3] at intervals of 0.1 ev, and from these a mean continuum cross section was calculated for each of the regions as a function of temperature. A correction factor[4] to account for plasma interactions was also included.

The computed radiative cross sections for all five regions are presented in Table 1 as a function of temperature. The model is further illustrated in Fig. 1 where the effective absorption cross section is shown as a function of photon energy $h\nu$. It should be noted that the temperature limitations on the present model are due to the fact that only transitions associated with nitrogen atoms were included. Below 8000–10,000°K molecular band radiation becomes important, whereas above 18,000–20,000°K bound-bound, bound-free, and free-free transitions involving N^+ and N^{++} may be important. These effects were not included in the present model.

It should also be noted that although only nitrogen radiative transitions were used in evaluating the absorption coefficients for the different regions of the step model, the results should still be applicable to air plasmas. This general use is justified from a practical viewpoint because nitrogen transitions dominate air radiative emission and absorption.

In order to test whether or not the present five-step model would be satisfactory for calculations of the integrated radiative intensity and heat flux in high-temperature air, comparisons were made between results obtained using this model and both the shock-tube data of Nerem and Stickford[5] and exact calculations provided by Wilson[6] of the Lockheed Palo Alto Research Laboratory. The shock-tube measurements corresponded to the integrated radiative intensity I over the wavelength region of 0.17–6 μ. Excellent agreement was shown to exist between these data and calculations using the present five-step model (only regions 1 and 2 contribute to the observed wavelength region). Satisfactory comparisons were also made with Wilson's results for all five regions of the spectrum. Thus, the five-step absorption coefficient model presented in Table 1 appears to represent a relatively simple approximation of the spectral characteristics of nitrogen or air while still retaining the essential nongray features.

In addition, comparisons were made with the previously noted shock-tube results of Golobic and Nerem.[1] The complete details of this experiment, including the problem of equilibrium in both the incident and reflected shock-wave regions, are discussed in Ref. 1. However, the primary results of Golobic and Nerem are summarized in Fig. 2. Here, the experimentally obtained end-wall radiative heat-transfer data corresponding to a time of 10 μsec after shock reflection are presented as a function of incident shock velocity. Calcu-

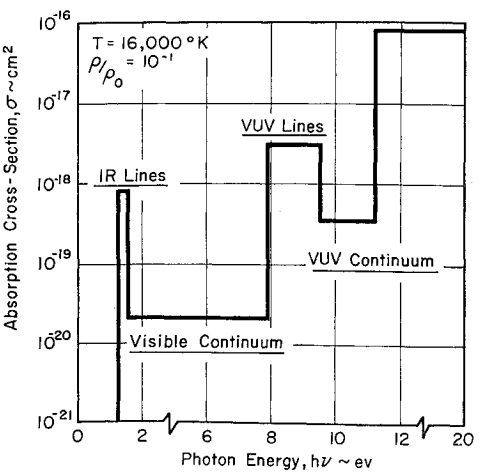

Fig. 1 Illustration of the five-step absorption cross-section model for typical conditions.

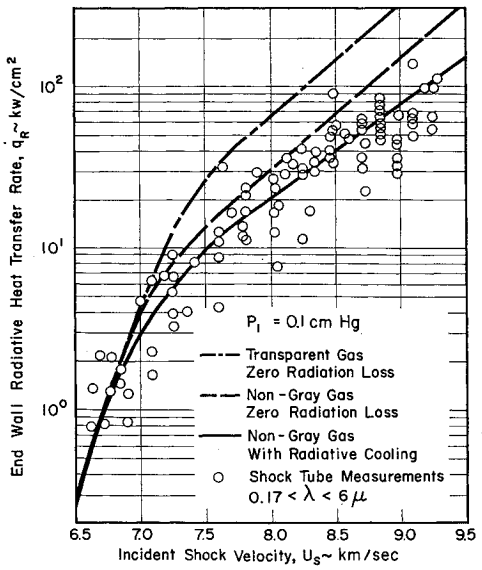

Fig. 2 Comparison of shock tube end-wall radiative heat-transfer rate measurements with calculations using five-step absorption coefficient model.

lated values obtained by using the present five-step absorption coefficient model in the numerical solution of Ref. 7 are also shown in this figure and reasonable agreement is seen to exist. This favorable comparison may be contrasted with that provided by the other two calculations shown in Fig. 2. The first is for an isothermal transparent slab (no radiative cooling or self-absorption), and the second includes only self-absorption (without radiative cooling). As may be seen, for the higher velocities the former is a factor of three and the latter approximately 50% greater than the mean of the data. It is only at the lowest velocities that these three calculations are in agreement. Thus, the effects of self-absorption and radiative cooling both appear to be important for the present conditions. Although the calculations shown in Fig. 2 suggest that self-absorption is the more important of these two effects, photomultiplier measurements of the radiative time-history behind reflected shock waves in air at these conditions indicate that significant radiative cooling is also present.

It should be noted that the present calculations are as much as 25–50% lower than the earlier two-step model calculations of Ref. 1, and are in reasonable agreement with the mean of the data. It should also be noted that a similar absorption coefficient model has been used by Page et al.[8] in carrying out theoretical calculations of stagnation-point radiative heat transfer at super-orbital velocities. Because of the similarities between the absorption coefficient models, the present agreement with experiment indirectly supports the calculations of Page et al.

References

[1] Golobic, R. A. and Nerem, R.M., "Shock Tube Measurements of End-Wall Radiative Heat Transfer in Air," *AIAA Journal*, Vol. 6, No. 9, Sept. 1968, pp. 1741–1747.

[2] Weise, W. L., Smith, M. W., and Glennon, B. M., "Atomic Line Transition Probabilities, Hydrogen Through Neon," Vol. 1, NBS Rept. NSRDS-NBS4, May 1966, National Bureau of Standards.

[3] Wilson, K. W. and Nicolet, W. E., "Spectral Absorption Coefficients of Carbon, Nitrogen, and Oxygen Atoms," Rept. 4-17-66-5, Nov. 1965, Lockheed Missiles & Space Co., Palo Alto, Calif.

[4] Armstrong, B. H., "Apparent Positions of Photoelectric Edges and the Merging of Spectral Lines," *Journal of Quantitative Spectroscopy & Radiative Transfer*, Vol. 4, 1964, pp. 207–214.

[5] Nerem, R. M. and Stickford, G. H., "Shock Tube Studies of Equilibrium Air Radiation," *AIAA Journal*, Vol. 3, No. 6, June 1965, pp. 1011–1018.

[6] Wilson, K. H., private communication, 1967, Lockheed Palo Alto Research Lab.

[7] Anderson, J. D., "Radiative Transfer Effects on the Flow Field and Heat Transfer Behind a Reflected Shock Wave in Air," *The Physics of Fluids*, Vol. 10, No. 8, Aug. 1967, pp. 1785–1793.

[8] Page, W. A. et al., "Radiative Transport in Inviscid Non-adiabatic Stagnation-Region Shock Layers," AIAA Paper 68-784, Los Angeles, Calif., 1968.

Thermal Transport and Relaxation Processes in Shock-Heated Argon

KLAUS WILLEKE* AND DANIEL BERSHADER†
Stanford University, Stanford, Calif.

THIS Note reports the results of experiments on high-temperature thermal transport and ionization relaxation in argon. The measurements were made with an improved thin-film surface thermometer[1] located in the end wall of the Stanford Aerophysics Laboratory high-pressure shock tube and were intended to constitute an independent check on similar studies made by the optical interferometric technique.[2] Measurement of temperature as a function of time following shock reflection yielded heat-transfer rates from the wall thermal layer in a temperature range not attained previously with this type of device.

The resistance thermometer heat gage consists of a triple-layered element (40 Å Cr–400 Å Pt–400 Å Cr) coated by a somewhat thicker layer of SiO_2 (8000 Å). The coating is chemically matched to the quartz (SiO_2) substrate such that the sensor is embedded essentially in a homogeneous medium. Its response to a heat input at the gage surface is then obtainable by means of a simple transfer function.

Figure 1 shows the heat-gage response in argon. The first rise occurs upon shock reflection from the end wall and is caused by the sudden deposition of energy into the translational mode of the gas. All internal degrees of freedom are "frozen" for some time, typically a few microseconds for present experimental conditions. Equilibrium ionization is attained at the end of a characteristic relaxation time. The latter stages of the approach to equilibrium are quite rapid. Consequent modification of the thermochemical state of the gas produces a corresponding effect on the thermal transport and, therefore, on the wall temperature behavior. The latter change is seen as the second rise in Fig. 1. That figure, therefore, contains information on 1) heat transfer from the non-ionized gas at "frozen" temperatures in excess of 1 ev, 2) re-

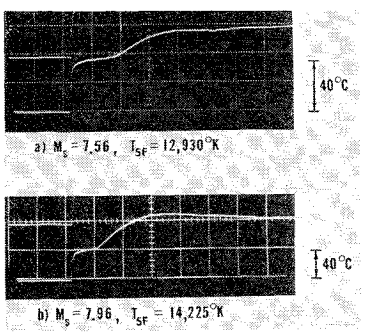

Fig. 1 Response of end-wall heat-transfer gage in argon; P_1 = 10 torr, T_1 = 297°K, sweep speed = 50 μsec/div; T_{5F} represents "frozen" temperature of the non-ionized gas behind the reflected shock.

Received June 23, 1969. This work was supported by NASA Grant NGR-05-020-091.

* Research Fellow; presently Postdoctoral Fellow at the Institut für Plasmaphysik, Garching bei München, West Germany. Member AIAA.

† Professor of Aerophysics and Associate Chairman, Department of Aeronautics and Astronautics. Associate Fellow AIAA.